International Journal of Advanced Multidisciplinary Research and Studies

Evaluation of Nonlinear Viscosity Property in a Magnetized Micropolar Fluid Flow, Experiencing Slip, and Convective Heating Properties

[1] **Olumuyiwa A Agbolade**, [2] **Ephesus O Fatunmbi**
[1, 2] Department of Mathematics and Statistics, Federal Polytechnic, Ilaro, Nigeria

Corresponding Author: **Olumuyiwa A Agbolade**

Abstract

The impact of nonlinear dynamic fluid characteristics on the magnetized motion of the micropolar fluid is explored in the current work. The transport phenomenon is configured on a vertical lengthening plate influenced by thermal radiation, wall slip, and convective heating properties. A mathematical model is set up to describe the problem practically and then converted from the initial partial into ordinary derivatives of order three using a similarity transformation approach. Thence, a numerical tool is sought for the solution of the transformed model for appropriate discussion of results. The outcomes of the numerical solution are represented graphically and deliberated upon for usage in various industrial and engineering operations. It is found that there exists a shrinking thermal boundary layer and momentum boundary structure as the Prandtl number enhances. Hence, a cool surface is found with a higher Prandtl number, and the flow velocity is reduced as well. A depreciation of the momentum boundary layer structure occurs as the viscosity variation term enhances.

1. Introduction

The indispensability offered by non-Newtonian fluids in the processes of engineering and industry has made the investigation of their properties so interesting and practical. Some of these fluids are colloids, molten polymers, paints, synovial fluids, biological fluids, suspensions, etc. (Turkyilmazoglu, 2016; Sajid *et al.*, 2009) [18, 17]. The nature of these fluids is quite different from the Newtonian fluids in many ways: the nonlinearity of the stress-strain relationship, the complexity of their configuration, their shear thinning and thickening properties, etc. Their wide applications include the fields of oil drilling, food and drug manufacturing, paint rheology, crude oil extraction, biomedical engineering, etc. Given their complexity, various models of these fluids have been derived in the literature because of the inability of a single model to contain all their characteristics. Some of the various types of these fluids are the micropolar type, Casson type, Geseskus type, Johnson Segemal type, and Powell-Eyring type, to mention a few. Of all the various non-Newtonian fluids that exist, the micropolar fluid stands out due to its ability to describe fluids with a microstructure that characterizes both translatory and spinning properties simultaneously. Eringen (1966, 1972) [6, 7] was the first to formulate the constitutive equations for this kind of fluid, including the thermal conduction of its properties. Liquid crystals, polymeric fluids, lubricants, and colloids, including animal blood, characterize the micropolar type of non-Newtonian fluid. Its applications in biomedical engineering, crude oil extraction, pharmacodynamics, food production, etc., have motivated many researchers to investigate various aspects of its thermophysical properties in different configurations. For instance, Lukaszewicz (1999) [14] gave a comprehensive application of micropolar fluid. Ahmad *et al.* (2011) derived a numerical model for the micropolar fluid experiencing the prescribed wall frictional force, laminar flow, and steady flow with mixed convective properties towards a stagnation point. The authors discussed two solutions for the cooled surface and the heated plate. An extension of Ahmad *et al.*'s work is found in Hsiao (2017) [12], where the author evaluates the impact of nanofluid and viscous dissipation on the transport of micropolar fluid. The mathematical setup, which was solved by the finite difference numerical technique, incorporated the Brownian motion and thermophoresis influence for the heat-mass transfer properties of the fluid.

The investigation of fluid flow alongside heat transfer when the viscosity is constant has been found to be inaccurate in many fields of engineering. For instance, hot rolling, nuclear power plants, heat exchanger systems, etc. There is a connection between the temperature and the viscosity; the variation in the temperature distribution in the floe regime induces a variation in the viscosity. Hence, it is of importance to investigate the thermal-dependent property of the viscosity for the overall prediction of the system. Such a problem has been explored by various scholars on various geometries and using different conditions.

Ahmad *et al*. (2018) [2] investigated such a phenomenon on a Casson fluid over a porous extending plate, and Fatunmbi and Adeniyan (2018) [8] evaluated such a concept on a micropolar fluid experiencing thermal and velocity wall slip. Fatunmbi *et al*. (2023) discussed the nonuniform viscosity condition in the flow of a micropolar fluid consisting of microorganisms over an extending sheet. Other related works can be found in due to the inspiration derived from the above literature, the current work intends to explore the impact of nonlinear viscosity, thermal radiation, slip, and convective heating properties in the flow of a magnetized micropolar fluid in the presence of non-constant thermal conductivity. Applications of this study can be encountered in the food processing industries, paper production, textile manufacturing, drying processes, heat exchanger systems, and heat transfer thermal devices. The resultant equations are tackled by a numerical algorithm of shooting and Runge-Kutta Fehlberg, and the results are presented using several graphs.

2. Problem Modelling and Analysis
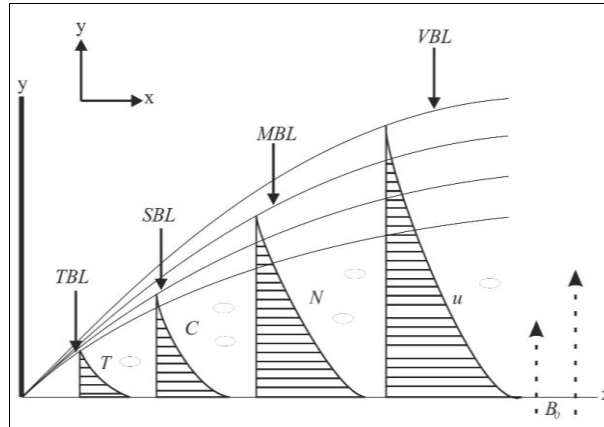
Fig 1: Flow Configuration

As depicted in Fig 1, the flow is hypothesised to be steady, non-turbulent and incompressible. The model consists of a dissipative and radiative micropolar fluid which flows over a two-dimensional plate experiencing thermophoresis and slip properties represented by $\beta \frac{\partial v}{\partial y}$ where β is connotes the slip length. The micropolar fluid is believed to be electroconductive with constantly imposed magnetic field at a normal angle to the motion of the fluid, The vortex viscosity is also taken to be constant but the other properties like the dynamic viscosity and the thermal conductivity are non-constant. No consideration for Hall currents, electric and induced magnetic fields in this analysis in this model. The sheet is subjected to surface mass flux with suction/injection velocity $V_w(x)$ with $V_w > 0$ indicates suction, while $V_w < 0$ indicates injection and $V_w = 0$ represents impermeable plate. The far-field thermal and solutal values are assumed to be T_∞ and C_∞ respectively while the boundary conditions at the surface are assumed to be convective thermal and convective solutal conditions with the plate surface being heated by convection with hot fluid of temperature T_f alongside the diffusion of chemical species. The expression of the equations appropriate for the problem at hand is based on the above-mentioned assumptions in connection with well-known boundary layer approximations. Therefore, the listed equations are the governing equations which describe the flow, thermal and solutal fields of the problem (Fatunmbi *et al*, 2023; Das *et al*, 2014 [5]; Das *et al*., 2015 [4]).

$$\frac{\partial u}{\partial x} + \frac{\partial v}{\partial y} = 0, \tag{1}$$

$$u\frac{\partial u}{\partial x} + v\frac{\partial u}{\partial y} = \frac{1}{\rho_\infty}\frac{\partial}{\partial y}\left(\mu\frac{\partial u}{\partial y}\right) + \frac{r}{\rho_\infty}\frac{\partial^2 u}{\partial y^2} + \frac{r}{\rho_\infty}\frac{\partial \omega}{\partial y} - \frac{\sigma_0 B^2(x)}{\rho_\infty}(u - U_0) \tag{2}$$

$$u\frac{\partial \omega}{\partial x} + v\frac{\partial \omega}{\partial y} = \frac{\gamma}{\rho_\infty j}\frac{\partial^2 \omega}{\partial y^2} - \frac{r}{\rho_\infty j}\left(2\omega + \frac{\partial u}{\partial y}\right) \tag{3}$$

$$u\frac{\partial C}{\partial y} + v\frac{\partial C}{\partial y} = Dm\frac{\partial^2 C}{\partial y^2} - k_r(C - C_\infty)^m - \frac{\partial}{\partial y}(V_T C) \tag{4}$$

$$u\frac{\partial T}{\partial x} + v\frac{\partial T}{\partial y} = \frac{1}{\rho_\infty c_p}\frac{\partial}{\partial y}\left[\left(\kappa + \frac{16T_\infty^3\sigma^*}{3k^*}\right)\frac{\partial T}{\partial y}\right] + \frac{(\mu+r)}{\rho_\infty c_p}\left(\frac{\partial u}{\partial y}\right)^2 + \frac{\sigma_0 B^2(x)(u-U_0)}{\rho_\infty c_p}u^2 + \frac{p'''}{\rho_\infty c_p}, \tag{5}$$

The boundary conditions are as follows:

$$U = \beta \frac{\partial U}{\partial y}, V = V(x)_w, \omega = -s \frac{\partial u}{\partial y}, -\kappa \frac{\partial T}{\partial y} = h_f(T_f - T), -Dm \frac{\partial C}{\partial y} = h_m(C_f - C) \text{ at } y = 0,$$

$$u = U_0, \omega \rightarrow 0, T = T_\infty, C = C_\infty \text{ as } y \rightarrow \infty. \tag{6}$$

The last term in equation (5), i.e., p''' indicates the non-uniform heat source or sink which is expressed as

$$p''' = \frac{\kappa_\infty U_0}{2x\, v_\infty} \left[\xi(T_f - T_\infty)e^{-\eta} + h(T - T_\infty) \right] \tag{7}$$

Similarly, μ is expressed as (see Lai and Kulacki, 1989; Kumari, 2001; Makinde, 2010)

$$\mu = \frac{\mu_\infty}{[1 + A(T - T_\infty)]}, \tag{8}$$

While κ is described as (see Chiam, 1996, Parida et al., 2015 [15])

$$\kappa = \kappa_\infty \left[1 + \Upsilon \left(\frac{T - T_\infty}{T_f - T_\infty} \right) \right]. \tag{9}$$

Furthermore, the Thermophoretic velocity V_T is expressed as

$$V_T = -\frac{k_t^*}{T_{ref}} \frac{\partial T}{\partial y}, \tag{10}$$

where k_t^* is described as

$$k_t^* = \frac{2Cs(\kappa/k_s + C_t K_n)(C_1 + C_2 e^{C_3/K_n})}{(1 + 3C_m K_n)(1 + 2\kappa/k_s + 2C_t K_n)}, \tag{11}$$

and the Thermophoretic parameter τ is defined as

$$\tau = -\frac{k_t^*(T_f - T_\infty)}{T_{ref}}. \tag{12}$$

2.1 Model Transformation
The variables in equation (13) are made use of in the governing equations for the purpose of transforming them into non-dimensional ordinary derivative:

$$\eta = y \left(\frac{U_0}{x v_\infty} \right)^{1/2}, \psi = (U_0 x v_\infty)^{1/2} f(\eta), \omega = U_\infty \left(\frac{U_0}{x v_\infty} \right)^{1/2} g(\eta), \gamma = \left(\mu + \frac{\mu_r}{2} \right) j, j = \frac{v_\infty x}{U_0},$$

$$\phi(\eta) = \frac{C - C_\infty}{C_w - C_\infty}, \theta(\eta) = \frac{T - T_\infty}{T_f - T_\infty} = \frac{T - T_r}{T_f - T_\infty} + a, a = \frac{T_r - T_\infty}{T_f - T_\infty}, u = \frac{\partial \psi}{\partial y}, v = -\frac{\partial \psi}{\partial x}. \tag{13}$$

On using the quantities stated in equation (13) in the governing Eqs. (2-5), equation. (1) is satisfied while the other equations (2-5) yield:

$$\left(\frac{a}{a - \theta} + K \right) f''' + \frac{a}{(a - \theta)^2} \theta' f'' + K g' + \frac{ff''}{2} - M^2(f' - 1) = 0, \tag{14}$$

$$\left(\frac{a}{a - \theta} + \frac{K}{2} \right) g'' + f'g + fg' - 2K(2g + f'') = 0, \tag{15}$$

$$\phi'' + Sc \left(\frac{f}{2} - \tau \theta' \right) \phi' - Sc\tau \phi \theta'' - (\zeta \phi) = 0. \tag{16}$$

$$(1 + \delta\theta + Nr)\theta'' + \delta\theta'^2 + \frac{Pr}{2} \left(1 - \frac{\theta}{a} \right)(1 + \delta\theta)f\theta' + PrEc \left(\frac{a}{a - \theta} + K \right) f''^2 +$$

$$PrEcM^2(f' - 1)^2 + (ae^{-\eta} + \beta\theta) = 0. \tag{17}$$

Also, the boundary conditions become

$$f'(0) = bf''(0), f(0) = fw, g(0) = -\beta f''(0), \theta'(0) + c\left(\frac{1-\theta(0)}{1+\delta\theta(0)}\right) = 0, \phi(0) = 1$$
$$f'(\infty) = 1 \; g(\infty) = 0, \theta(\infty) = 0, \phi(\infty) = 0.$$

(18)

with $K, M, fw, Pr, \delta, a, Ec, b, c, d, \alpha(\beta), Nr, Sc, \zeta, \tau$ being material(micropolar) parameter, Magnetic, suction/injection, Prandtl, thermal conductivity, viscosity variation, Eckert number, slip, thermal Biot number/surface convection, Solutal Biot number/solutal convective, thermal (space) dependent heat source/sink, radiation, Schmidt number, chemical rate of reaction, thermophoresis parameters respectively.

3. Numerical Solution and Verification of Generated Results

The nonlinearity exhibited by the system of the governing equations (14–18) has made it difficult to assess a closed-form solution to the present problem. Hence, the researchers are compelled to use a numerical tool via the Runge-Kutta-Fehlberg scheme for the solution. In this view, the solution to the nonlinear ordinary derivatives equations (14–17) along with their wall constraints is found by the shooting technique. This numerical tool is relevant to these equations owing to its nonlinearity and accuracy, as well as its unconditional stability. For a detailed description of this numerical tool, readers can check out Das *et al.* (2014) [5], Fatunmbi, and Okoya (2020) [10]. For the sake of the computations, the researchers have carefully selected the following values for the emerging parameters:
$K = 0.5, c = d = 0.3, \tau = 0.3, \beta = 0.4, \; Nr = 0.3, Ec == 0.2, Sc = 0.8, Pr = 0.72, \alpha = 0.2, M = 0.5$. However, individual graph has different values of the parameters which are varied to showcase the effects of the physical terms.

Table 1: Variation of M as its affects $-f''(0)$ in comparison with existing data

M	Mabood and Das (2016)	Xu and Lee (2012)	Current Results
0	1.000008	-	1.00000
1	1.4142135	1.41421	1.41421
5	2.4494987	2.4494	2.44949
10	3.3166247	3.3166	3.31662
50	7.1414284	7.1414	7.14143
100	10.049875	10.0498	10.04989
500	22.383029	22.3830	22.38302
1000	31.638584	-	31.63863

4. Discussion of Outcomes

The understanding of the behaviour of each of the crucial terms as they react with dimensionless profiles of velocity, temperature and concentration is important for valuable application in engineering and industrial works. Therefore, the consequence of the current research are presented in graphs to showcase the impacts of the included parameters. The presentation of the graphs is followed by relevant discussion of the results.
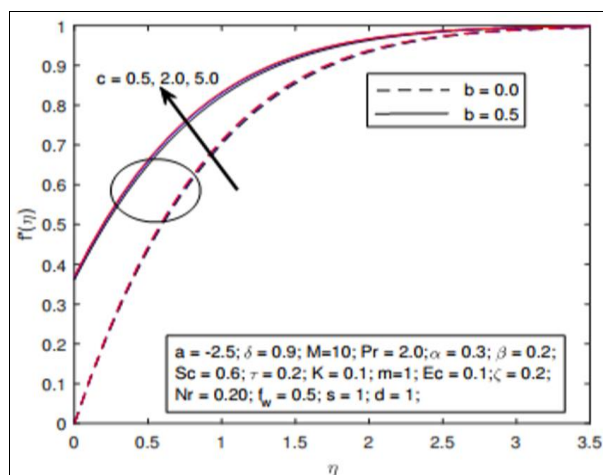
Fig 2: Nature of the velocity profile as c changes in magnitudes

Fig 2 is a description of variation in the trend of the velocity profiles as the surface convection parameter c changes in the presence of the slip term. There is an acceleration in the velocity field as c alters in magnitude. The hotness of the liquid break the bond of the dynamic viscosity as c increases and as such, the resistance to the fluid motion is reduced which in turn encourage a higher velocity. However, a thicker hydrodynamic structure is observed in the presence of the slip proprty b as found in this picture.
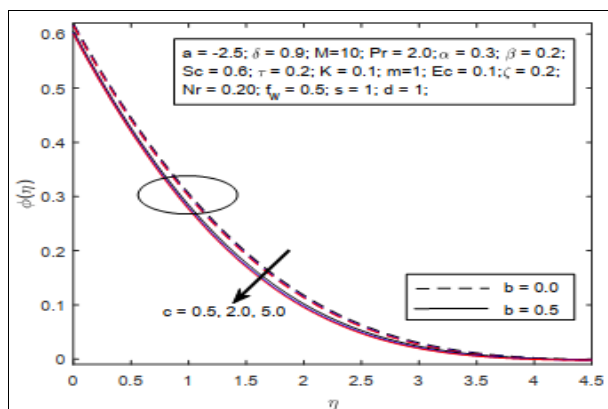
Fig 3: Thermal distribution for changes in the values of c

For fixed values of the other parameter and varying the values of c, the solutal behaviour is capture in Fig 3. It is noticed that there is a decrease in the solutal region as the surface convection term rises. A depreciation occurs in this field due to higher values of c. This observation is in harmony with that of Das *et al*. (2025). Additionally, there is a diminishing trend in the concentration distribution as the slip property b increases in values as noted in Fig 3.
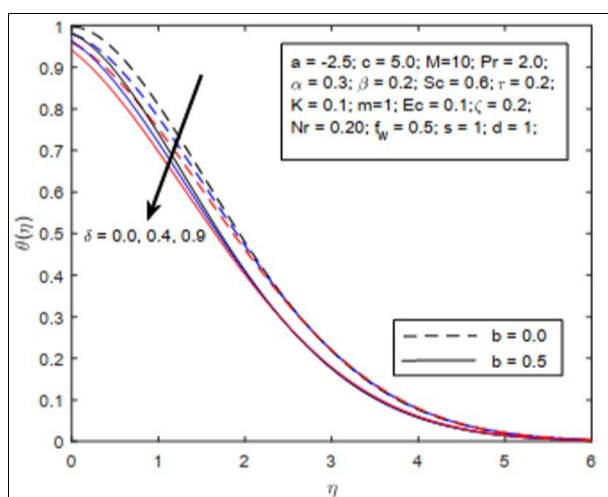
Fig 4: Nature of the thermal distribution for changes in δ

Fig 4 depicts the nature of the heat profiles as there is alterations in the values of δ which is the thermal conductivity term when other terms are fixed. It is noted that the presence or absence of the slip property does not hinder the downward trend of the heat profiles as δ increases in value. There is a depreciation in the thermal boundary layer structure which leads to a cool surface as δ progresses. This trend can be of useful result in various thermal devices that require cooling of the surface of the device.
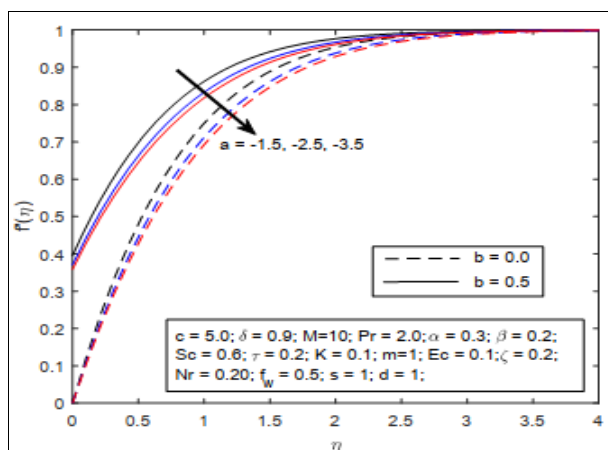
Fig 5: Nature of the velocity distribution for changes in a
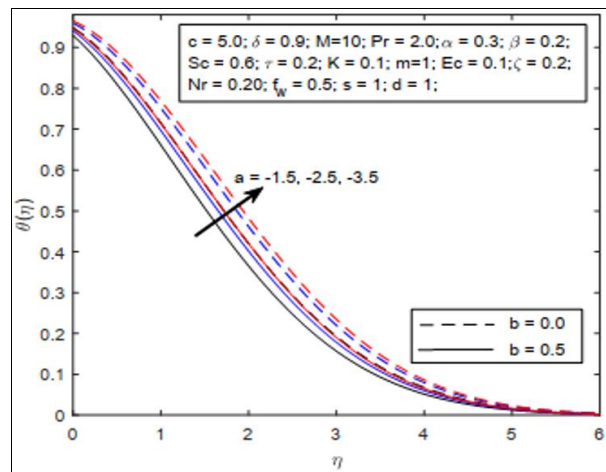
Fig 6: Thermal trend for changes in the viscosity term a

The viscosity variation term, which is symbolized by a is varied in the Fig 5 as the velocity profiles react against the distance η. A downward trend results from growing in the strength of a This is because the viscous force is higher thereby creating more resistance and drag in the micropolar fluid and consequently, a reduced velocity profile. The converse is the case for the thermal distribution as noted in Fig 6. There is a hike in the heat profile as a enhances. The drag created in the flow field generates friction in the system and thereby causes the temperature to appreciate as observed in Fig 6.
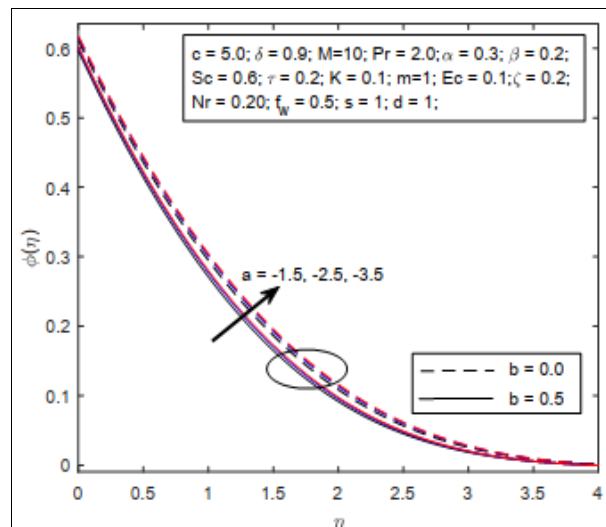
Fig 7: Concentration field for changes in the viscosity term a

In a similar manner, Fig 7 shows a description of the on-centration profile as a enhances. An upward trend is found as a increases. The drag created in the flow field induces friction in the system and thereby causes the concentration field to appreciate as can be seen in this figure.
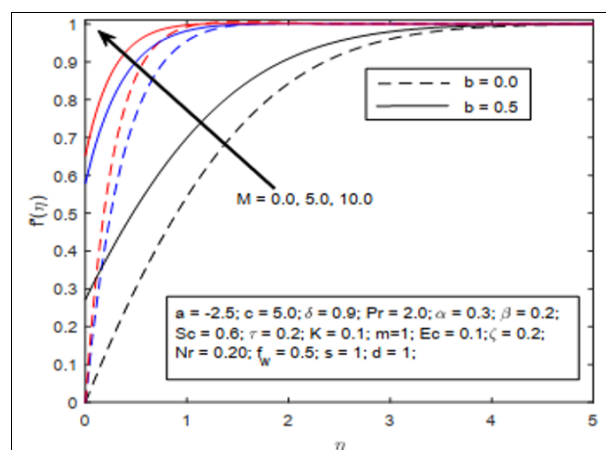
Fig 8: Trend of the velocity profile for alterations in M

The influence of M on the speed of the fluid is captured in Fig 8 in the presence and absence of b. It is of interest to note that there is a growth in the momentum boundary layer as M progresses as found in this shape. However, the thickness is more pronounced in the presence of b as clearly illustrated in this graph.
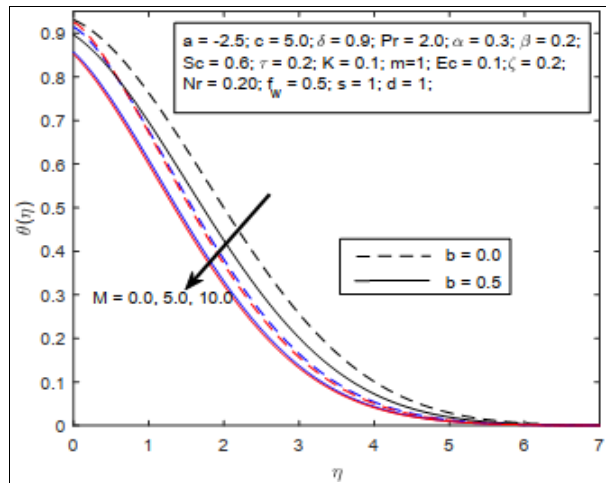
Fig 9: Trend of the temperature profile for altreations in M
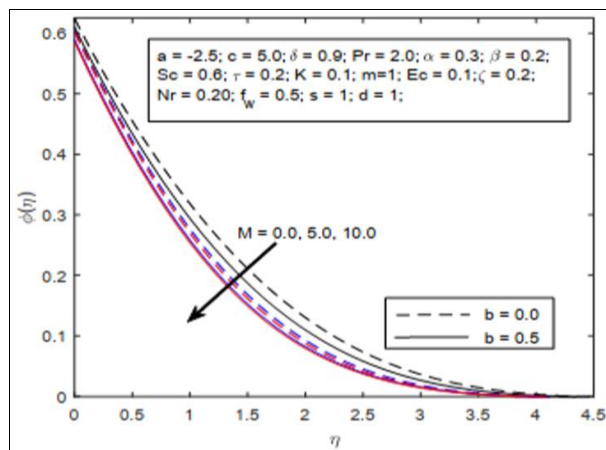
Fig 10: Trend of the concentration profile for altreations in M

The behaviours of M on both the heat and solutal fields are respectively described in Fig 9 and 10 in the presence and absence of the slip property b. Both dimensionless profiles $\theta(\eta)$ and $\phi(\eta)$ are found to depreciate as M is raised in value. It is of interest to note that there is a shrink thermal and solutal boundary structures as M progresses as found in this shape. However, the thickness is more pronounced in the presence of b as clearly illustrated in this graph.
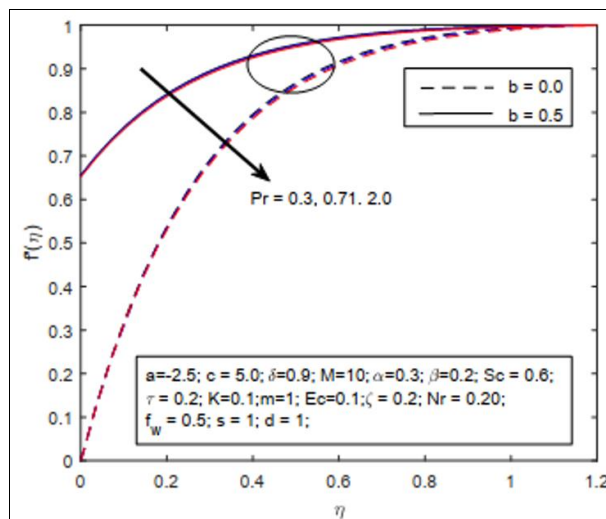
Fig 11: Reaction of velocity field as Pr changes in values

The reaction of the velocity field to various values of the Prandtl number is exhibited in Fig 11. A downward trend occurs as Pr rises in magnitude. This is due to the fact that Pr is in direct proportion to the micropolar fluid dynamic viscosity of the micropolar fluid, consequently, enhancing Pr corresponds to growth in the viscosity. Such a relationship strengths the dynamic viscosity and creates more resistance into the speed of the fluid and therefore a decrease in the motion.
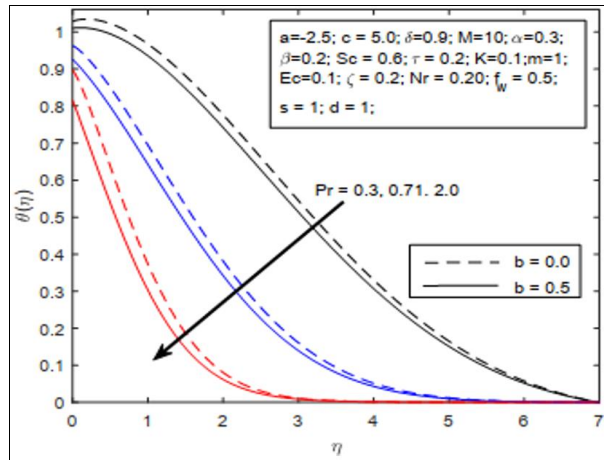
Fig 12: Thermal characteristics for changes in Pr

Fig 12 reveals the character of the thermal profiles for variation in Pr. Rising values of Pr propels a diminished thermal structure as noted. An increase in Pr reduces the temperature and cools the surface because tere is enhancement in the heat transfer with growth in Pr due to a reduced thermal conduction.
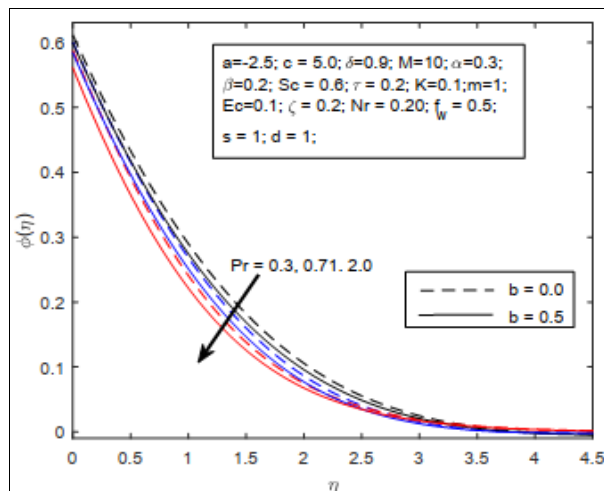
Fig 13: Nature of the concentration profile for alterations in Pr

A similar characteristic of Fig 12 is shown in Fig 13 for the reaction of Pr on the concentration profiles. As depicted in Fig 10, rising values of Pr leads to a depreciation of the solutal boundary layer structure which consequently causes a reduction in the concentration profiles.

4. Conclusion

In conclusion, this investigation explores the parametric effects of nonlinear viscosity, thermal radiation, slip, and convective heating properties on the flow of a magnitized micropolar fluid over an extending device. A mathematical model is set up to physically describe the phenomenon; the developed physical model is further scrutinized by relevant similarity quantities to yield third-order ordinary derivative equations, which are then solved by the Runge-Kutta Fehlberg algorithm with a shooting approach. In order to visualize the effects of the physical terms on the non-dimensional profiles of velocity, temperature, and concentration, graphs are plotted and the results discussed appropriately. The results are in harmony with previously published data in the literature in some limiting situations. It was found out that:

- There exists a shrinking thermal boundary layer and momentum boundary structure as the Prandtl number enhances. Hence, a cool surface is found with a higher Pr number, and the flow velocity is reduced as well.
- There is a depreciation in the hydrodynamic structure as the viscosity term improves in strength, which leads to a fall in the flow motion.
- The thermal and concentration fields appreciate significantly when the viscosity variation term is enhanced, but a cool surface is found for the enhancement of the thermal conductivity term.

5. References

1. Ahmad K, Nazar R, Pop I. Boundary layer flow and heat transfer of a micropolar fluid near the stagnation point on a stretching vertical surface with prescribed skin friction, International Journal of Minerals, Metallurgy and Materials. 2012; 18(4):502-508.
2. Ahmad K, Halim SA, Hanouf. Z. Variable Viscosity of Casson Fluid Flow Over a Stretching Sheet in Porous Media with Newtonian Heating, Journal of Informatics and Mathematical Sciences. 2018; 10(1 & 2):359-370.
3. Chiam TC. Heat transfer in a fluid with variable thermal conductivity over a linearly stretching sheet, Acta Mechanica. 1998; 129:63-72.
4. Das K, Jana S, Kundu PK. Thermophoretic MHD slip flow over a permeable surface with variable fluid properties, Alexandria Engineering Journal. 2015; 54:35-44.
5. Das K, Duari PR, Kundu PK. Numerical simulation of nanofluid flow with convective boundary condition, Journal of the Egyptian Mathematical Society, 2014. Doi: http://dx.doi.org/10.1016/j.joems.2014.05.009
6. Eringen AC. Theory of micropolar fluids, J. Math. Mech. 1966; 16:1-18.
7. Eringen AC. Theory of Thermo-Microfluids. Journal of Mathematical Analysis and Applications. 1972; 38:480-496. Doi: doi.org/10.1016/0022-247X(72)90106-0
8. Fatunmbi EO, Adeniyan A. Heat and Mass Transfer in MHD Micropolar Fluid Flow over a Stretching Sheet with Velocity and Thermal Slip Conditions, Open Journal of Fluid Dynamics. 2018; 8:195-215.
9. Fatunmbi EO, Oke AS, Salawu SO. Magnetohydrodynamic micropolar nanofluid flow over a vertically elongating sheet containing gyrotactic microorganisms with temperature-dependent viscosity, Results in Materials. 2023; 19:p100453.
10. Fatunmbi EO, Okoya SS. Heat transfer in boundary layer magneto-micropolar Fluids with temperature-dependent material properties over a stretching sheet, Advances in Materials Science and Engineering, 2020, Article ID 5734979, 11 pages. Doi: https://doi.org/10.1155/2020/5734979
11. Fatunmbi EO, Ramonu OJ, Salawu SO. Analysis of heat transfer phenomenon in hydromagnetic micropolar nanoliquid over a vertical stretching material featuring convective and isothermal heating conditions, Waves in Random and Complex Media, 2023. Doi: https://doi.org/10.1080/17455030.2023.2173494
12. Hsiao K. Micropolar nanofluid flow with MHD and viscous dissipation effects towards a stretching sheet with multimedia feature, International Journal of Heat and Mass Transfer. 2017; 112:983-990.
13. Kumar L. Finite element analysis of combined heat and mass transfer in hydromagnetic micropolar flow along a stretching sheet. Comput Mater Sci. 2009; 46:841-848.
14. Lukaszewicz G. Micropolar Fluids: Theory and Applications, Birkhauser, Basel, 1999.
15. Parida SK, Panda S, Rout BR. MHD boundary layer slip flow and radiative nonlinear heat transfer over a flat plate with variable fluid properties and thermophoresis, Alexandria Engineering Journal. 2015; 54:941-953.
16. Qasim M, Khan I, Shafie S. Heat Transfer in a Micropolar Fluid over a Stretching Sheet with Newtonian Heating, PLoS ONE. 2013; 8(4):1-6.
17. Sajid M, Abbas Z, Hayat T. Homotopy analysis for boundary layer flow of a micropolar fluid through a porous channel, Applied Mathematical Modelling. 2009; 33:4120-4125.
18. Turkyilmazoglu M. Flow of a micropolar fluid due to a porous stretching sheet and heat transfer, International Journal of Non-Linear Mechanics. 2016; 83:59-64.